Mimp, a Mitochondrial Carrier Homologue, Inhibits Met-HGF/SF-Induced Scattering and Tumorigenicity by Altering Met-HGF/SF Signaling Pathways

Raya Leibowitz-Amit,[1] Galia Tsarfaty,[2,3] Yamit Abargil,[1] Gil M. Yerushalmi,[1] Judith Horev,[1] and Ilan Tsarfaty[1]

[1]Department of Human Microbiology, Sackler Faculty of Medicine, Tel-Aviv University, Tel Aviv, Israel; [2]Van Andel Research Institute, Grand Rapids, Michigan; and [3]Sheba Medical Center, Tel Hashomer, Israel

Abstract

We have recently shown that Mimp, a mitochondrial carrier protein homologue, is induced by Met-hepatocyte growth factor/scatter factor (HGF/SF) signaling and decreases the mitochondrial membrane potential in DA3 mammary adenocarcinoma cells. We show here that induction of Mimp leads to growth arrest in response to HGF/SF by arresting cells at the S phase of the cell cycle. Induction of Mimp or its transient expression does not lead to apoptosis. Mimp also attenuates HGF/SF-induced cellular scattering *in vitro* and tumor growth *in vivo*. The exogenous induction of Mimp at levels similar to its endogenous induction by HGF/SF increases the level of the Met protein and its phosphorylation by HGF/SF but reduces the levels of Shc and prevents the HGF/SF-induced tyrosine phosphorylation of Grb2 and Shc. In contrast, the level of phosphatidylinositol 3-kinase (PI3K) increases following Mimp induction and the level of phosphorylated PI3K in response to HGF/SF is unaffected by the exogenous induction of Mimp. Moreover, exogenous Mimp prevents the HGF/SF-induced transcription of the *serum response element-luciferase* reporter gene. Our results show that Mimp expression reduces Met-HGF/SF-induced proliferation and scattering by attenuating and altering the downstream signaling of Met. These data show a new link between a tyrosine kinase growth factor receptor and a mitochondrial carrier homologue that regulates cellular growth, motility, and tumorigenicity. (Cancer Res 2006; 66(17): 8687-97)

Introduction

Met, a heterodimeric receptor tyrosine kinase, is expressed in a wide variety of normal and malignant cells. Activation of Met by its ligand hepatocyte growth factor/scatter factor (HGF/SF) can lead to many different biological outcomes, including proliferation, cell survival, scattering, invasion, and angiogenesis as well as differentiation and apoptosis (1). The Met-HGF/SF signaling pathway has been implicated in physiological processes of embryonic development and differentiation as well as in pathological cancerous transformation and metastasis (2).

Binding of HGF/SF to Met leads to autophosphorylation of several tyrosine residues in the tyrosine kinase domain of the receptor and at its docking site (3). The multisubstrate docking site of Met recruits adapter signaling molecules, such as Grb2, Shc, Gab1, and Crk/CRKL (4), and signaling transducers, such as phosphatidylinositol 3-kinase (PI3K), signal transducer and activator of transcription 3 (Stat3), phospholipase Cγ, and Src (5). Recruitment of Shc and Grb2 (either directly or indirectly) to the Met docking site has been implicated in Ras activation and Met-induced proliferation and migration (6). The p85 regulatory subunit of PI3K can associate directly with Met or through the adapter protein Gab1 (7), and its activation has been implicated in Met-HGF/SF-induced protection from apoptosis (8).

Recently, we reported the cloning of a novel gene, designated *mimp* (Met-induced mitochondrial protein), which is up-regulated in NIH 3T3 cells constitutively expressing both Met and HGF/SF (9). Mimp was shown to be induced by the signaling pathway of Met-HGF/SF in several cell lines, among them, the murine adenocarcinoma cell line DA3. Mimp is expressed in a wide range of tissues with an expression pattern similar to that of Met (9). *Mimp*, which is also designated mitochondrial carrier homologue 2, was identified in cDNA libraries of $CD34^+$ hematopoietic stem/progenitor cells (10) and in expressed sequence tag libraries of mouse blastocysts (11). It was also purified from mitochondria of normal heart tissue (12), verifying its mitochondrial localization. In addition, *mimp* mRNA was increased 2-fold in human skeletal muscle in response to insulin (13) and was recently shown to be a target of tBID in cells signaled to die by tumor necrosis factor α (14).

Mimp encodes a 33-kDa protein that has sequence and structural homology to the family of mitochondrial carrier proteins and was shown to localize to the mitochondria (9, 14). Mimp and another novel gene product, designated presenilin-associated protein [PSAP, also known as mitochondrial carrier homologue 1 (mtch1); ref. 15], form a subfamily of mitochondrial carrier homologues, having 47% identity and 65% similarity in their amino acid sequences. Recently, PSAP was shown to be a proapoptotic mitochondrial protein and was suggested to be involved in presenilin-1-regulated apoptotic cell death cascades (16).

Our previous work showed that exogenous induction of Mimp leads to mitochondrial depolarization in Mimp-inducible DA3 (iMimp-DA3) cells (9). We now present a detailed characterization of the effect of Mimp on the cellular phenotype of DA3 cells and on their biological response to HGF/SF. Our results show that induction of Mimp attenuates the cellular response to HGF/SF in terms of growth and motility *in vitro* and in terms of tumorigenicity *in vivo*, in parallel with alterations in the Met signaling cascade.

Note: This work was carried out in partial fulfillment of the requirements for the Ph.D. degrees of R. Leibowitz-Amit and G.M. Yerushalmi.

Requests for reprints: Ilan Tsarfaty, Department of Human Microbiology, Sackler Faculty of Medicine, Tel-Aviv University, Tel Aviv 69978, Israel. Phone: 972-3-6407015; Fax: 972-3-6409160; E-mail: ilants@post.tau.ac.il.

©2006 American Association for Cancer Research.

doi:10.1158/0008-5472.CAN-05-2294

Downloaded from http://aacrjournals.org/cancerres/article-pdf/66/17/8687/2552059/8687.pdf by guest on 05 March 2024

Materials and Methods

Cells. DA3 (17), iMimp-DA3 (9), T47D, MDA-MB-231, MDA-MB-435, 9L (obtained from American Type Culture Collection, Bethesda, MD), and 293T cells were grown in DMEM supplemented with 10% heat-inactivated FCS (Life Technologies, Gaithersburg, MD). The generation of iMimp-DA3 cells was described elsewhere (9). Mimp was induced in these cells by incubation with different concentrations of the tetracycline derivative doxycycline (Sigma, St. Louis, MO). In general, all of the cell experiments *in vitro* were done in triplicate or quadruplicate and repeated at least four times.

Plasmids, reagents, and commercial antibodies. The cloning of Mimp and the construction of pEGFP-C1 (Clontech, Palo Alto, CA) and pcDNA3.1 and pcDNA3.1-His (Invitrogen, Carlsbad, CA) fusion vectors were described elsewhere (9). The protein products of these plasmids are designated GFP-Mimp, pcDNA-Mimp, and pcDNA-Mimp-His, respectively. Recombinant human HGF/SF was purified from the supernatant of transfected NIH 3T3 cells that overproduce this growth factor (18). HGF/SF concentrations are presented as scatter units/mL determined by the ability of the factor to scatter Madin-Darby canine kidney cells (MDCK) cells (units/mL). The mitochondrial membrane potential (MMP)–sensitive dye JC-1 was purchased from Molecular Probes (Eugene, OR).

The antibody used for immunoprecipitation was PY20 anti-phosphotyrosine (Transduction Laboratories, Lexington, KY). The primary antibodies used for Western blot were monoclonal anti-polyhistidine (dilution 1:3,000; Sigma), monoclonal anti-Grb2 (dilution 1:500; Transduction Laboratories), mouse monoclonal anti-cdc2 (Santa Cruz Biotechnology, Santa Cruz, CA), monoclonal anti-actin (dilution 1:1,500; Chemicon, Temecula, CA), polyclonal anti-p27 (dilution 1:1,000; Cell Signaling, Danvers, MA), and polyclonal antibodies anti-Met (dilution 1:200), anti-PI3K (dilution 1:200), anti-Shc (dilution 1:200), and anti-p21 (dilution 1:800; all from Santa Cruz Biotechnology). The secondary antibodies were horseradish peroxidase (HRP)–conjugated anti-rabbit IgG (1:40,000) and anti-mouse IgG (1:20,000; both from Jackson ImmunoResearch Laboratories, West Grove, PA). The primary antibodies used for immunofluorescence were mouse monoclonal anti–cytokeratin 19 (dilution 1:10; Amersham, Piscataway, NJ) and 6H2.B4 mouse monoclonal anti–cytochrome *c* (PharMingen, San Diego, CA), and the secondary antibody used was FITC-conjugated donkey anti-mouse IgG (dilution 1:150; Jackson ImmunoResearch Laboratories).

Generation of polyclonal anti-Mimp antibodies. The *Mimp-pET28a* plasmid was transformed into BL21 (DE3) pLysS-competent bacteria, and Mimp-His expression was induced by isopropyl-L-thio-β-D-galactopyranoside (IPTG; 1 mmol/L) for 3 hours. The bacterial pellet was lysed under denaturing conditions [8 mol/L urea, 0.1 mol/L NaH_2PO4, Tris-HCl (pH 8.0)], and the protein was extracted from the denatured supernatant on Ni^{+2-}NTA beads according to the protocols of Qiagen (Chatsworth, CA). Protein lysates were analyzed by Western blot using anti-histidine antibodies for the appearance of the purified protein detected as a band at a size of ~33 kDa. The fractions containing the protein underwent dialysis against decreasing concentration of urea. After obtaining sufficient purified protein, two rabbits were immunized with an emulsion of purified protein and complete Freund's adjuvant according to the protocols detailed in ref. 19. When the appearance of Mimp-specific antibodies was detected and no increase in antibody titer occurred between two consecutive injections, the rabbits were exsanguinated. For purification, the sera were absorbed with lyophilized BL21 bacterial powder to get rid of antibodies generated against bacterial epitopes and then further purified with ammonium sulfate (19). The titer of anti-Mimp antibodies in the sera was assessed by Western blot, and the sensitivity and specificity of the antibody were determined (results not shown).

DNA transfection and 4′,6-diamidino-2-phenylindole staining. Cells were transiently transfected using the Lipofectin reagent kit (Life Technologies) as suggested by manufacturer. For visualization of the nucleus, cells were fixed with cold absolute methanol for 10 minutes, permeabilized with cold acetone for 10 minutes, and stained with 4′,6-diamidino-2-phenylindole (DAPI; Sigma) for 20 minutes.

Cell viability assay. Cell viability was measured using the crystal violet cell staining technique (20). Briefly, cells were grown with different concentrations of doxycycline and HGF/SF for 5 days in 96-well plates. Cells were then washed with PBS, fixed with 4% paraformaldehyde, and stained with a dye containing 0.1% crystal violet in H_2O for 20 minutes. Cells were then destained under running water for ~30 minutes and lysed in 0.2% Triton X-100 for 2 hours, and the absorbance was measured at 595 nm. For determination of the cellular doubling time, 10^4 cells were plated in identical plates and counted during the 5 following days. The slope of the graph depicting the logarithm of the number of cells in time was extrapolated by regression and the doubling time was calculated as log 2/slope.

Cell cycle and apoptosis analysis. For assessing cell cycle distribution, DA3 cells were synchronized at G_0 following growth in starvation medium (0.1% FCS in DMEM) for 48 hours. Cells were then seeded with or without doxycycline (100 ng/mL) and allowed to grow for 5 days. HGF/SF was added to the growth medium for the last 24 hours, and the cells were fixed in 70% ethanol, washed, stained with 50 μg/mL propidium iodide (PI; Sigma), and analyzed using the fluorescence-activated cell sorting (FACS; FACSort, Becton Dickinson, Franklin Lakes, NJ). For double staining with PI and bromodeoxyuridine (BrdUrd), BrdUrd was added to the medium of growing cells 1 hour before fixation, and the preparation of cells for FACS analysis was done using a special cell proliferation kit (Amersham). FITC-conjugated goat anti-mouse IgG (Jackson ImmunoResearch Laboratories) was used as the secondary antibody and PI was added at the final stage. For assessing apoptosis, cells were grown without synchronization with doxycycline and HGF/SF and then fixed and stained with PI. As a positive control for apoptosis, cells were either irradiated with UV light (254 nm) at 18 J/m^2 or treated with 1 μmol/L staurosporine as described previously (21).

Serum response element-luciferase assay. iMimp-DA3 cells were plated in 24-well plates and cotransfected with the *serum response element (SRE)-luciferase (SRE-LUC)* reporter plasmid and the internal control *phRL-TK* plasmid carrying the *Renilla* luciferase gene. Doxycycline was added for 3 days, and HGF/SF (80 units/mL) was added for an additional 24 hours. Cells were lysed and cell lysates were processed by using the Dual-Luciferase Assay kit (Promega, Madison, WI) according to the manufacturer's protocol. The luciferase activity was normalized relative to *Renilla* for each well and the average value of six wells was compared with transfected nontreated cells.

Scatter assay. iMimp-DA3 and DA3 cells were grown with different concentrations of doxycycline for 2 days to allow for Mimp expression, harvested, and seeded in a scatter assay as described previously (22, 23). HGF/SF was added to quadruplicate wells in serial dilutions of two, starting from a concentration of 8,000 units/mL. Cells were allowed to grow overnight and were then fixed with methanol, air-dried, and stained with Giemsa. The concentration of HGF/SF that no longer led to cell scattering was documented by two independent observers who were unaware of the experimental setup.

Generation and measurements of tumors *in vivo*. *In vivo* tumorigenicity of the parental DA3 cells and iMimp-DA3 cells was assessed by orthotropic injection of 10^6 cells to the mammary pads of 20 female BALB/C mice (6-8 weeks old). Ten mice from each group received regular water and 10 mice received water containing 2 mg/mL doxycycline. Mice were monitored for tumor growth once weekly by caliper measurement and ultrasonographic measurement using a 15L8 linear transducer (15 MHz, Acuson, Mountain View, CA). Gray-scale sonography was done every 7 days over 21 days, and each animal was evaluated for tumor presence, size, and location. Imaging settings were standardized and unchanged throughout the experiment. No major near-field artifacts were encountered. Images were obtained by experienced sonographers who were unaware of the treatment status of the animals. The *in vivo* experiment was done thrice with almost identical results. All the animal work fully complied with the Van Andel Research Institute Institutional Animal Care and Use Committee requirements.

RNA preparation, Northern blot analysis, and cDNA array analysis. RNA was prepared using the Tri-reagent kit (Sigma) and RNA concentration was measured by absorbance at 260 nm. Northern blotting was done as described in Sambrook et al. (24). The radioactive ^{32}P DNA probe was prepared using a purified PCR product of Mimp with the NEBlot kit

Downloaded from http://aacrjournals.org/cancerres/article-pdf/66/17/8687/2552059/8687.pdf by guest on 05 March 2024

(New England Biolabs, Beverly, MA). For gene expression analysis, RNA was reverse transcribed and the cDNA was radioactively labeled and hybridized to a broad coverage "Atlas" 1.2 array containing 1176 genes according to the manufacturer's instructions (Clontech).

Immunoprecipitation and Western blot analysis. For cell signaling experiments, cells were grown with 100 and 500 ng/mL doxycycline for 2 days, serum starved for 24 hours, and then treated with HGF/SF (80 units/mL) for 20 minutes. Near-confluent cells were washed and lysed in 1 mL lysis buffer [20 mmol/L Tris-HCl (pH 7.8), 100 mmol/L NaCl, 50 mmol/L NaF, 1% NP40, 0.1% SDS, 2 mmol/L EDTA, 10% glycerol] with protease inhibitor cocktail (Roche Molecular Biochemicals, Mannheim, Germany) and 1 mmol/L sodium orthovanadate. Protein concentration was quantified using the BCA protein assay kit (Pierce, Rockford, IL). For immunoprecipitation, 250 μg total protein was incubated with 1 μL anti-phosphotyrosine antibody overnight at 4°C with gentle rocking and precipitated with 40 μL of 50% protein A-Sepharose in PBS (Amersham Biosciences, Uppsala, Sweden). The beads were pelleted, washed thrice in PBS, and finally taken up in 50 μL SDS loading buffer for gel electrophoresis. For Western blot analysis, 30 μg cell lysate protein was evaluated. Visualization was achieved using HRP-conjugated anti-rabbit or anti-mouse IgG, enhanced chemiluminescence reaction, and exposure to X-ray film (Kodak, Rochester, NY). Usually, the same membrane was subjected to several consecutive experiments following stripping with a fresh solution of Ponceau (0.2% Ponceau in a solution of 3% trichloroacetic acid in H_2O).

Immunofluorescence staining. For anti–cytokeratin 19 staining, Lab-Tek chamber slides (Nunc, Roskilde, Denmark) were plated with 10^4 iMimp-DA3 cells per well following treatment with doxycycline for 2 days and incubated for 24 hours with and without HGF/SF. The slides were fixed with cold absolute methanol for 10 minutes, permeabilized with cold acetone for 10 minutes, blocked in 1% bovine serum albumin and 10% normal donkey serum in PBS for 10 minutes, incubated with primary antibody for 1 hour at room temperature, washed thrice, stained with FITC-conjugated donkey anti-mouse antibody for 1 hour at room temperature, and washed again six times. Slides were mounted with coverslips using GelMount (Biomeda, Foster City, CA). For anti–cytochrome *c* staining, cells were grown with doxycycline for 24 hours, fixed with 4% paraformaldehyde for 30 minutes, permeabilized with 0.1% Triton X-100 for 10 minutes, and then blocked and stained using the same protocol.

Confocal analysis. Cells were analyzed using a 410 Zeiss (Obercocen, Germany) confocal laser scanning microscope with the following configuration: 25 mW krypton/argon (488 and 568 nm) and HeNe (633 nm) laser lines.

FACS analysis of MMP. Transfected 293T cells were analyzed for MMP as described previously (25). Briefly, a MMP-sensitive dye JC-1 was diluted to a final concentration of 5 μmol/L with prewarmed (37°C) culture medium and then added to cells at 37°C in the dark for 90 minutes. As a positive control for mitochondrial depolarization, 100 μmol/L carbonyl cyanide *m*-chlorophenylhydrazone (Sigma) was added to the incubation medium. The stained cells were washed, trypsinized, washed again, and resuspended in 1 mL PBS. The cells were analyzed by FACS with an argon laser with excitation at 488 nm and using filters transmitting at 525 ± 20 nm in the FL1 channel (green) and 590 nm in the FL2 channel (red). The ratio of red (593 nm) versus green (532 nm) fluorescence intensity was calculated for each cell and plotted as a histogram. The average fluorescence ratio of the cell population was calculated and normalized relative to nontransfected cells as control.

Data analysis and statistics. RNA and protein densitometry was done using the ImageJ software designed by the NIH (downloaded from http://rsb.info.nih.gov/ij/). Statistical analysis was done with the statistical tool kit in the Microsoft Excel software (Microsoft, Redmond, WA).

Results

Characterization of Mimp induction in iMimp-DA3 cells. We have reported previously the generation of an inducible system based on DA3 mammary adenocarcinoma cells, in which Mimp is induced by the antibiotic doxycycline (9). We used the Mimp-specific antibody we have generated to show that the addition of doxycycline to the growth medium leads to induction of the Mimp protein. Actin served as an internal loading control to the experiment, and densitometric analysis and normalization of the Mimp/actin ratio relative to noninduced cells allowed quantification of the extents of induction (Fig. 1*A*). We then compared the levels of endogenous induction of Mimp by HGF/SF and the levels of its exogenous induction by doxycycline at both the mRNA and the protein levels. 18S rRNA and actin served as internal loading controls to the experiments, respectively (Fig. 1*B* and *C*). The level of *mimp* mRNA increased in response to HGF/SF, doxycycline, and their combination as shown previously (9). The increase in *mimp* mRNA in response to doxycycline was dose dependent (Fig. 1*B*). In contrast, the extent of Mimp protein induction in the presence of 100 ng/mL doxycycline was similar to its endogenous induction by HGF/SF and did not further increase in the presence of 500 ng/mL doxycycline (Fig. 1*C*).

Effect of Mimp induction on cellular growth. To study the effect of Mimp induction on cellular growth, iMimp-DA3 cells were plated with different concentrations of doxycycline for 5 days in the presence or absence of HGF/SF. Cell number was assessed using the crystal violet cell staining assay (Fig. 2*A*). Mimp induction alone did not alter cellular growth. Interestingly, whereas HGF/SF led to a small nonsignificant increase in cell number in noninduced cells, it led to a significant inhibition of growth in Mimp-induced cells. The extent of the inhibition was dependent on the dose of doxycycline (Fig. 2*A*).

For determining the cellular doubling time, iMimp-DA3 cells were plated with varying concentrations of doxycycline with or without HGF/SF and then counted at different time points for 1 week. The doubling time of Mimp-inducible cells increased from ~21 to 26 or 29 hours in presence of 200 or 500 ng/mL doxycycline, respectively (Fig. 2*B*). HGF/SF treatment did not lead to a significant change in the cellular doubling time in noninduced cells but brought about a major increase in the cellular doubling time in Mimp-induced cells at doxycycline concentrations of 500 ng/mL (59 hours; Fig. 2*B*). Doxycycline treatment did not affect cell number or doubling time in either the absence or the presence of HGF/SF in the parental noninducible DA3 cell line (results not shown). These results indicate that inducible Mimp itself only slightly increases the cellular doubling time but leads to a significantly prolonged doubling time in response to HGF/SF.

These results brought us to compare the levels of endogenous Mimp in several other Met-expressing cell lines that differ in their proliferative response to HGF/SF. Three human breast cancer cell lines T47D, MDA-MB-231, and MDA-MB-435 and the rat glioma cell line 9L were grown in the presence and absence of HGF/SF for 5 days, and cell number was assessed using the crystal violet cell staining method. In parallel, total cellular protein was produced from identical plates and subjected to Western blot using the anti-Mimp polyclonal antibodies. In the glioma cell line 9L, HGF/SF led to proliferation; in the three breast cancer cell lines, it led to a decrease in cell number (Fig. 2*C*). Interestingly, the amount of endogenous Mimp was significantly lower in 9L than in the other three cell lines. In contrast, an increase in the levels of Mimp protein in response to HGF/SF was observed only in 9L cells (Fig. 2*D*).

Effect of Mimp induction on cell cycle. Cell cycle analysis was done following staining with PI. In the parental noninducible cells, the percentage of cells in the S phase of the cell cycle was increased 24 hours following HGF/SF treatment, and addition of doxycycline

Downloaded from http://aacrjournals.org/cancerres/article-pdf/66/17/8687/2552059/8687.pdf by guest on 05 March 2024

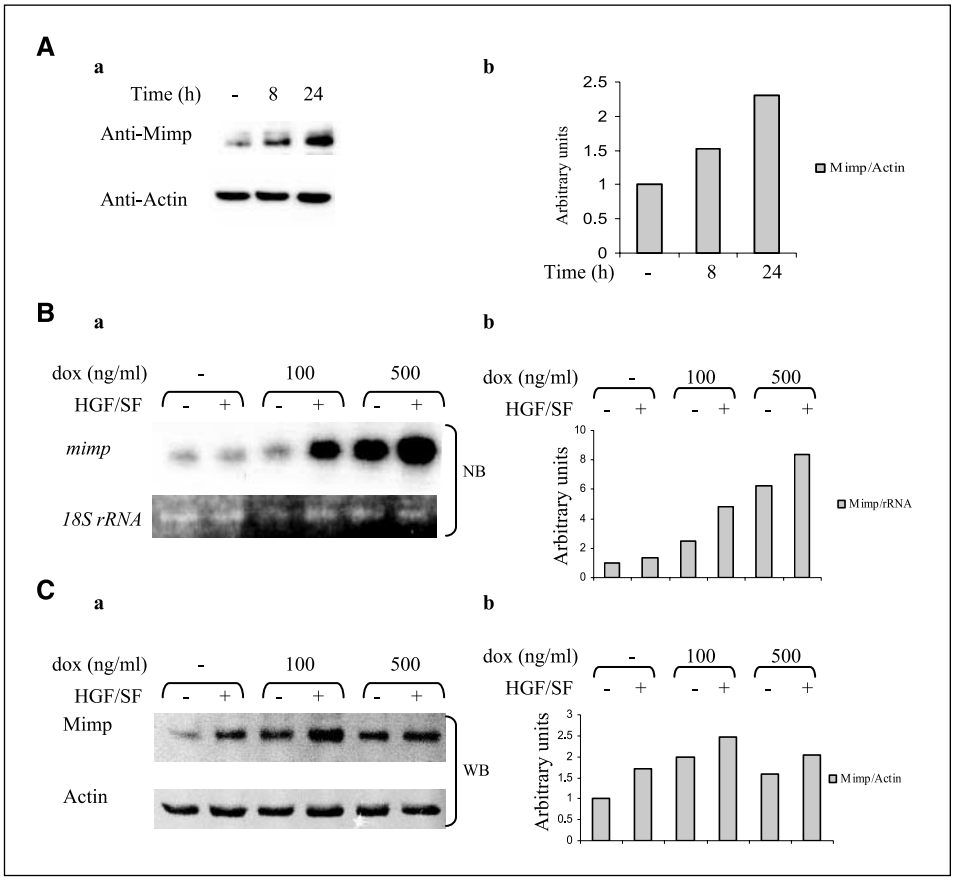

Figure 1. Time and dose response of Mimp induction in iMimp-DA3 cells. *A, a,* time response of Mimp induction following 0, 8, and 24 hours of treatment with 100 ng/mL doxycycline using the anti-Mimp polyclonal antibody. Actin served as an internal loading control. *b,* densitometric quantification of Mimp/actin ratio normalized relative to noninduced cells. *B, a,* Northern blot analysis of iMimp-DA3 treated with 0, 100, and 500 ng/mL doxycycline (*dox*) for 2 days and then treated with HGF/SF for 24 hours using a mimp-specific probe. rRNA served as an internal loading control. *b,* densitometric quantification mimp/rRNA ratio normalized relative to noninduced nontreated cells. *C, a,* Western blot analysis using extracts generated from identical plates as in (*B*) using the anti-Mimp polyclonal antibody. Actin served as an internal loading control. *b,* densitometric quantification Mimp/actin ratio normalized relative to noninduced nontreated cells.

did not alter the cell cycle distribution (Fig. 3*A, a*). In the iMimp-DA3 cells, HGF/SF treatment had the same effect on the cell cycle as in the control cells in the absence of doxycycline. Mimp induction at 100 ng/mL doxycycline led to a significant increase in the percentage of cells in S phase, and HGF/SF treatment of Mimp-induced cells led to a profound increase in the percentage of cells in S phase (Fig. 3*A, b*). Next, double staining with PI and BrdUrd was done, because PI staining allows monitoring of the cell cycle

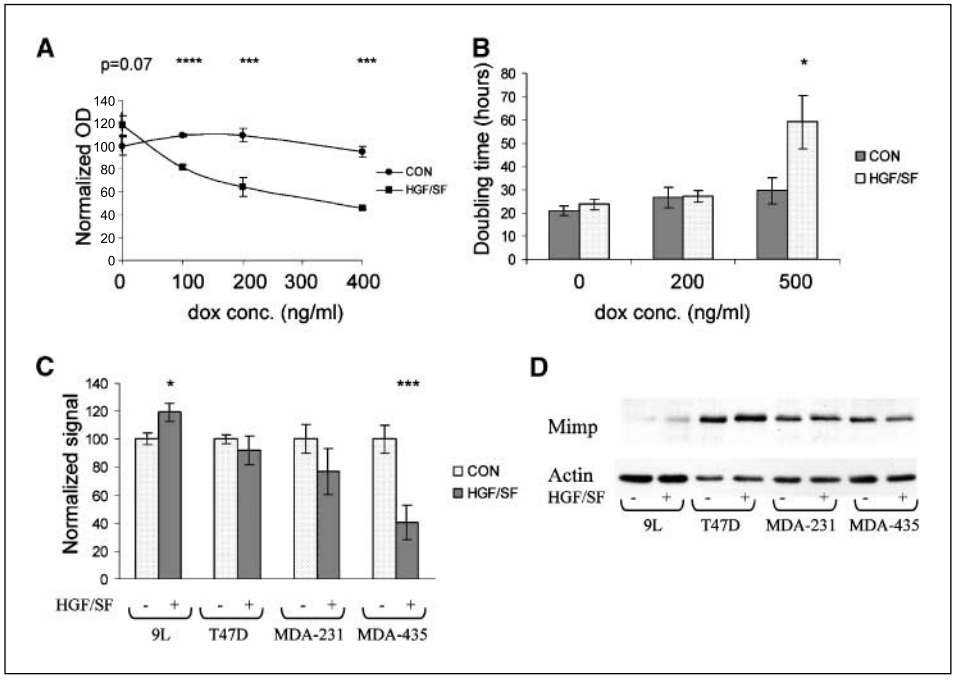

Figure 2. Mimp leads to growth retardation in response to HGF/SF. *A,* iMimp-DA3 cells were grown in the presence of varying concentrations of doxycycline with or without HGF/SF (80 units/mL) for 5 days. Cell number was determined using the crystal violet cell staining technique. The absorbance was normalized relative to control noninduced cells. *B,* doubling time of iMimp-DA3 cells was determined with and without HGF/SF in the presence of different concentrations of doxycycline. *C,* 9L, MDA-MB-231, MDA-MB-435, and T47D cells were grown in the presence and absence of HGF/SF for 5 days and the cell number was determined using the crystal violet cell staining technique. The absorbance was normalized for each cell line relative to control nontreated cells. *D,* total cellular protein was produced from identical plates as in (*C*) and subjected to Western blot using anti-Mimp antibodies. The amount of total cellular actin served as an internal loading control. *, $P < 0.05$; **, $P < 0.01$; ***, $P < 0.005$; ****, $P < 0.001$.

Downloaded from http://aacrjournals.org/cancerres/article-pdf/66/17/8687/2552059/8687.pdf by guest on 05 March 2024

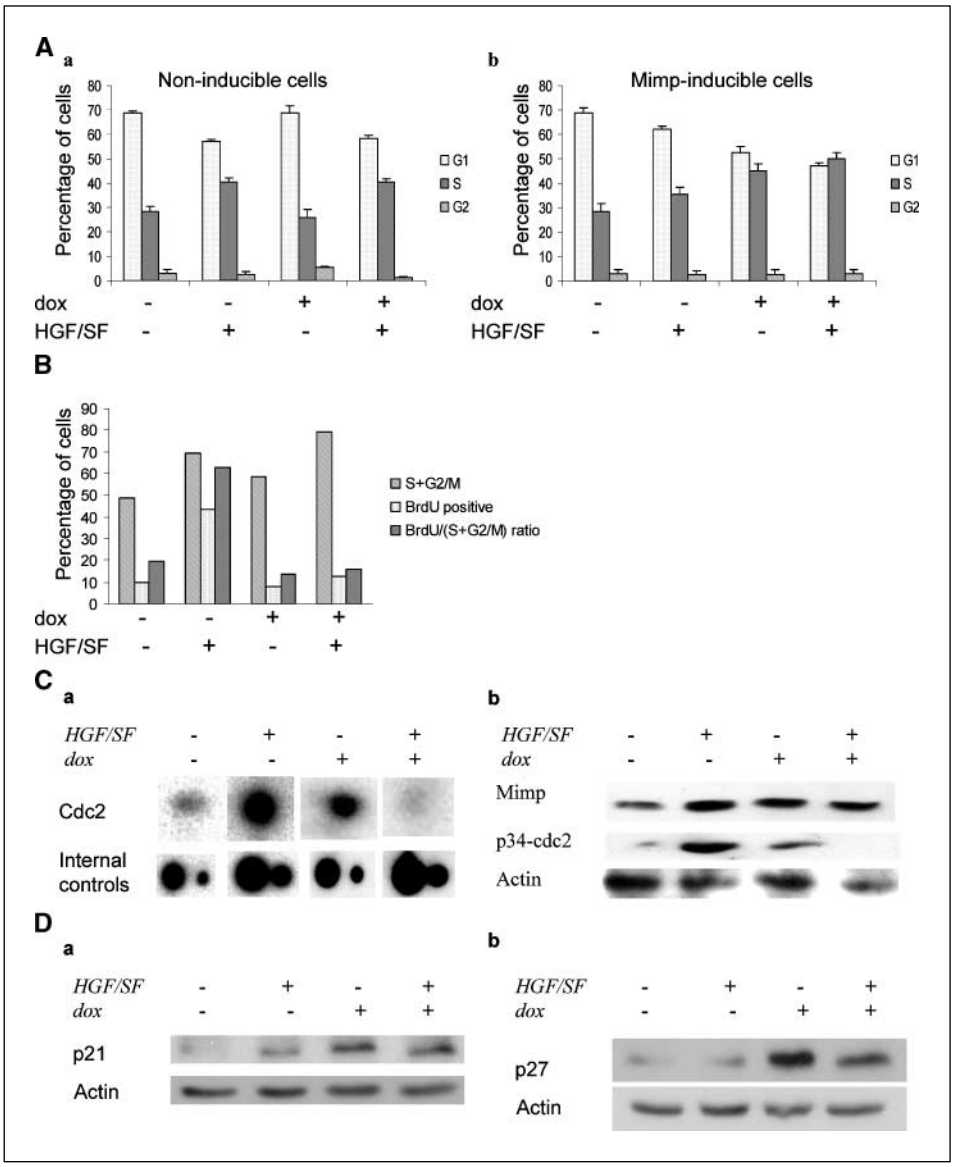

Figure 3. Mimp leads to S-phase arrest in response to HGF/SF. *A,* noninducible cells (*a*) and iMimp-DA3 cells (*b*) were grown in presence of 100 ng/mL doxycycline for 4 days, and HGF/SF was added for another 24 hours. Cell cycle distribution was analyzed after fixation and staining with PI. *B,* double staining with BrdUrd and PI was done for iMimp-DA3. The percentage of cells at the S and G_2-M phases and the percentage of BrdUrd-positive cells for each cell sample were determined. The ratio between the latter and the former was calculated. *C, a,* "Atlas" membranes were hybridized with mRNA extracted from cells with and without doxycycline and HGF/SF and then washed and exposed to X-ray film. The internal controls served to monitor the length of exposure time of each membrane. *b,* Western blot analysis of protein lysates from the same cells using anti-Mimp, anti-cdc2, and anti-actin antibodies. *D,* Western blot analysis of protein lysates from the same cells using anti-p21 (*a*) and anti-p27 (*b*) antibodies. The amount of total cellular actin served as an internal loading control.

distribution of the cells, whereas BrdUrd staining detects the subpopulation of cells that are actively synthesizing DNA. This analysis shows that the increase in the percentage of cells at the S phase in response to HGF/SF treatment was accompanied by an increase in the percentage of BrdUrd-positive cells (Fig. 3*B*). Under these conditions, the BrdUrd-positive cells accounted for 63% of all cells at the S and G_2-M phases relative to only 20% under control conditions. However, the increase in S phase occurring in response to Mimp induction and to HGF/SF treatment in the presence of Mimp was not accompanied by an increase in the percentage of BrdUrd-positive cells (Fig. 3*B*). These results suggest that both HGF/SF and Mimp drive DA3 cells into S phase, whereas HGF/SF treatment leads to active DNA synthesis and Mimp induction leads to accumulation of cells in S phase (i.e., DNA synthesis is inhibited or altogether arrested). This effect is greatly enhanced when HGF/SF is given to Mimp-expressing cells.

Gene expression analysis using "Atlas" cDNA arrays was done to determine which cell cycle transcripts are altered during the S-phase arrest. Surprisingly, the level of *cdc2* mRNA was increased in response to HGF/SF in absence of Mimp but was significantly decreased in response to HGF/SF in the presence of Mimp (Fig. 3*C, a*). Western blot analysis showed the same pattern of expression at the protein level (Fig. 3*C, b*). In contrast, the levels of the cell cycle inhibitors p21 and p27 were elevated in the presence of Mimp irrespective of HGF/SF treatment (Fig. 3*D*).

Mimp induction does not lead to apoptosis. We have shown previously that Mimp localizes to the mitochondria and decreases the MMP in iMimp-DA3 cells (9). Because a decrease in mitochondrial potential is an early event in apoptosis (26), we assessed whether induction of Mimp leads to apoptosis. Direct observation of cells induced to express Mimp for long periods did not reveal any morphologic features characteristic of apoptosis, such as membrane blebbing, cellular rounding, or nuclear fragmentation (results not shown). We determined the percentage of cells at the sub-G_0 peak as a measurement of apoptosis. HGF/SF treatment decreased the percentage of cells at the sub-G_0 peak by ~3-fold in noninduced cells. Induction of Mimp had no significant effect on the percentage of cells at the sub-G_0 peak both without and with HGF/SF (Fig. 4*A*).

Downloaded from http://aacrjournals.org/cancerres/article-pdf/66/17/8687/2552059/8687.pdf by guest on 05 March 2024

To study the effect of Mimp induction on the cellular susceptibility to apoptosis, noninduced and Mimp-induced cells were exposed to UV light at a dosage known to induce apoptotic cell death (8) 24 hours before cell fixation. UV irradiation led to an accumulation of cells at the sub-G_0 peak in both noninduced and Mimp-induced cells in a similar extent (Fig. 4*B* and *C*). Figure 4*B* shows representative histograms of the cells in the four different conditions, and Fig. 4*C* depicts the average percentage of cells at the sub-G_0 peak in the absence and presence of doxycycline in nonirradiated and in UV-irradiated cells. UV irradiation for a longer period increased the percentage of sub-G_0 cells in both noninduced and Mimp-induced cells without a significant difference between these two cell populations (results not shown). In concordance with this observation, a cytoplasmic DNA ladder, characteristic of cells undergoing apoptosis, was not apparent in the noninduced or Mimp-induced cells but was observed in the UV-irradiated cells under both conditions (results not shown). Last, the effect of Mimp induction on the subcellular localization of cytochrome *c* was studied using immunofluorescence. In both noninduced and Mimp-induced cells, cytochrome *c* was localized to the mitochondria without being released to the cytoplasm (Fig. 4*D*). This result further corroborates our observation that Mimp induction does not lead to apoptosis.

It was recently published that PSAP, which carries 47% identity and 65% similarity to Mimp, localizes to the mitochondria and leads to apoptosis following transient transfection into 293T (16). We therefore checked whether Mimp leads to apoptosis in a transient transfection assay. *pEGFP-Mimp*-transfected cells, which showed mitochondrial staining as observed previously (9), had normal cellular morphology with a flattened appearance. In contrast, cells in which apoptosis was chemically induced by staurosporine showed a rounded morphology typical of cells undergoing programmed cell death. In addition, nuclear staining of *pEGFP-Mimp*-transfected cells with DAPI following fixation showed that the nuclei were large, round, and intact, whereas in the staurosporine-treated cells the nuclei looked condensed (Fig. 5*A*).

293T cells were transiently transfected with an empty *pcDNA* vector, *pcDNA-Mimp*, or *pcDNA-Mimp-His* plasmid. The transfection was verified by Western blot analysis with anti-His antibodies (Fig. 5*B*). Transient transfection with Mimp or Mimp-His did not increase the percentage of cells at the sub-G_0 peak of the cell cycle relative to cells transfected with the empty *pcDNA* vector or to control nontransfected cells (Fig. 5*B, b*). Interestingly, transient transfection of 293T with *pcDNA-Mimp* or *pcDNA-Mimp-His* led to mitochondrial depolarization as shown previously for DA3 cells (9). The average red/green fluorescence JC-1 ratio of Mimp-transfected or His-Mimp-transfected cells was lower than the average ratio in control cells or cells transfected with the empty vector (Fig. 5*C*). These results show that although Mimp leads to a decrease in the MMP when transiently expressed in 293T it does not lead to cellular apoptosis.

Mimp induction attenuates HGF/SF-induced scattering. One of the well-documented responses of several cell lines, including DA3, to HGF/SF is cellular scattering (27). To study the effect of Mimp induction on scattering, iMimp-DA3 cells were plated in the presence of 100 or 500 ng/mL doxycycline for 2 days to allow for Mimp expression and then harvested and plated in quadruplicate

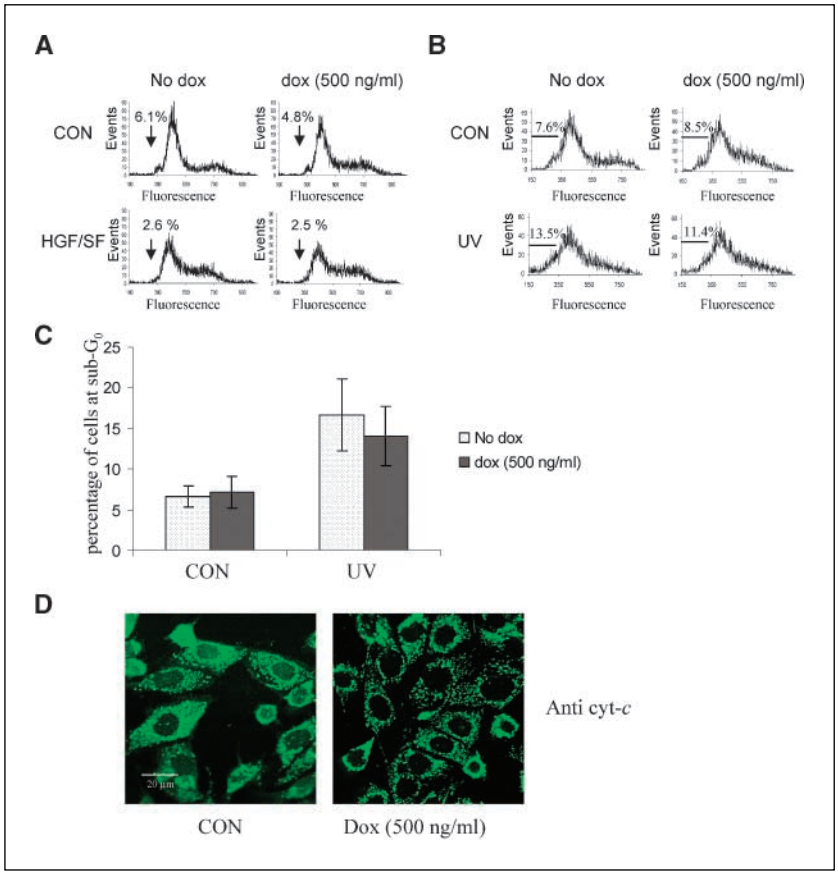

Figure 4. Mimp does not lead to apoptosis but decreases mitochondrial potential. *A,* iMimp-DA3 cells were grown with or without doxycycline (500 ng/mL) for 2 days and then treated with HGF/SF for 24 hours. Cell cycle distribution was analyzed after fixation and staining with PI and the percentage of cells at the sub-G_0 peak of the cycle was calculated. *B,* iMimp-DA3 cells were grown with or without doxycycline (500 ng/mL) and then exposed to UV irradiation and monitored for cell cycle distribution after 24 hours. Cell cycle distribution was analyzed after fixation and staining with PI and the percentage of cells at the sub-G_0 peak of the cycle calculated. *C,* average percentage of cells as the sub-G_0 peak of the cell cycle in each of the four conditions described in (*B*). *D,* iMimp-DA3 cells were treated with 500 ng/mL doxycycline and then subjected to immunofluorescence using anti–cytochrome *c* (*cyt-c*) antibodies.

Downloaded from http://aacrjournals.org/cancerres/article-pdf/66/17/8687/2552059/8687.pdf by guest on 05 March 2024

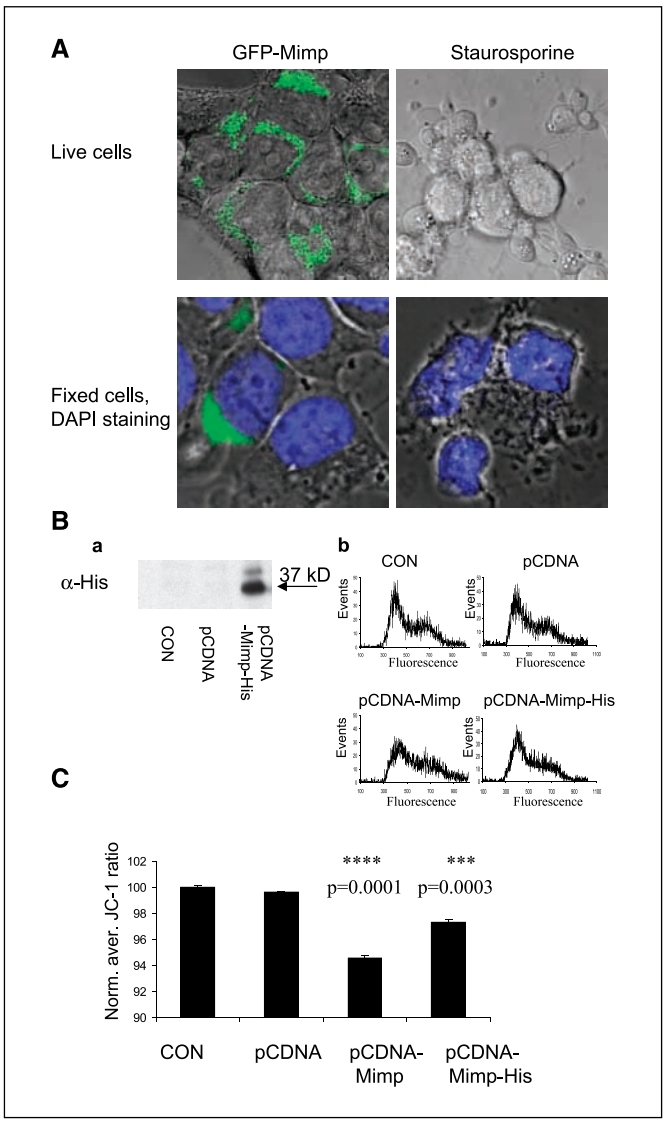

Figure 5. Mimp does not lead to apoptosis in 293T cells when transiently expressed. *A,* 293T cells were transfected with *pEGFP-Mimp* or treated with 1 mmol/L staurosporine. After 24 hours, their morphology was assessed using the confocal laser scanning microscope. Micrographs show live cells (*top*) or fixed cells after staining with DAPI (*bottom*). *B, a,* Western blot analysis of cell lysates from control cells or from cells transfected with *pcDNA* or *pcDNA-Mimp-His* using anti-His antibody. *b,* cell cycle distribution of control cells and cells transfected with *pcDNA, pcDNA-Mimp,* or *pcDNA-Mimp-His. C,* control nontransfected 293T or cells transfected with *pcDNA, pcDNA-Mimp,* or *pcDNA-Mimp-His* were stained with the mitochondrial membrane sensitive dye JC-1, and the average red/green fluorescence ratio of each cell population was calculated and normalized relative to the average ratio of nontransfected cells.

in the presence of serial dilutions of HGF/SF (see Materials and Methods for details). In control cells, the scattering effect of HGF/SF disappeared at a concentration of 1 unit/mL, whereas in the presence of Mimp the scattering effect of HGF/SF was no longer apparent at concentrations of 4 units/mL. Representative micrographs of cells grown in the presence of 2 units/mL HGF/SF are seen in Fig. 6*A*, which show that in presence of 500 ng/mL doxycycline Mimp-inducible cells grew in patches, whereas in the absence of doxycycline these cells were dispersed separately in the plate and showed a distinct spindle morphology. This could not be attributed to an effect of the antibiotic itself, as doxycycline treatment of the parental DA3 cells did not prevent their scattering in response to HGF/SF (Fig. 6*A*).

For further analyzing cellular morphology, cells were induced to express Mimp for 2 days and then harvested and seeded again in the presence of HGF/SF for 24 hours. Cells were fixed and part of the cytoskeletal network visualized by staining with an antibody against cytokeratin-19, an intermediate filament known to be expressed extensively in the cytoplasm of epithelial cells (28). As reported previously for MDCK (29), HGF/SF treatment of non-induced cells altered cellular morphology and cellular distribution of cytokeratin-19 (Fig. 6*B*). Control nontreated cells exhibited a rounded morphology, in which cytokeratin-19 formed a homogenous cytoplasmatic mesh. HGF/SF treatment led to cellular polarization, with cells having a typical spindle shape and two long cytoplasmatic extensions. Cytokeratin-19 was mainly dispersed around the nuclei and in those extensions (Fig. 6*B*). Induction of Mimp altered the HGF/SF-induced polarization and redistribution of cytokeratin-19. At doxycycline concentrations of 500 ng/mL, cells treated with HGF/SF had more rounded and less "spindle-like" morphology, and the cytokeratin-19 was distributed throughout the cytoplasm in a "mesh-like" pattern (Fig. 6*C*). These results indicate that Mimp attenuates HGF/SF-induced changes in cellular morphology, which are an essential step in the process of cellular migration and scattering.

Induction of Mimp decreases tumor growth *in vivo*. iMimp-DA3 and DA3 cells were injected into the mammary pads of female BALB/c mice. The mice were then divided arbitrarily to two

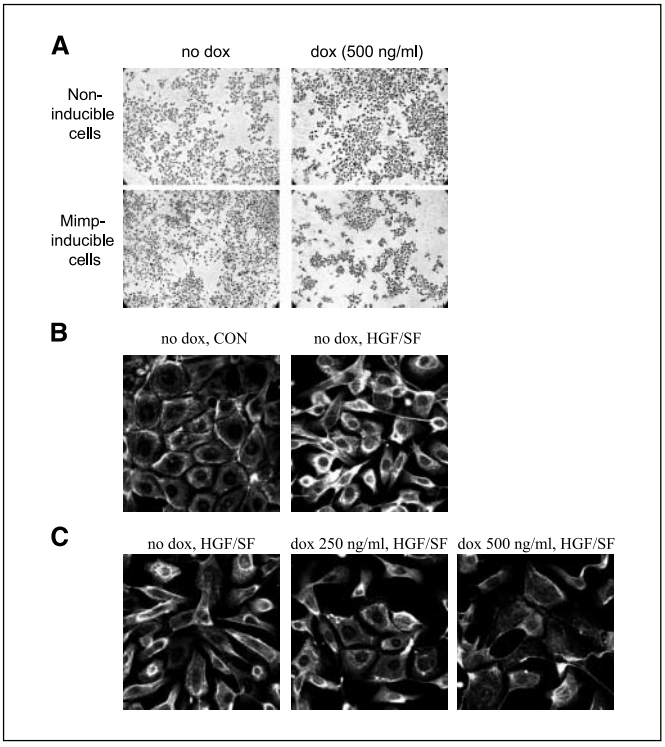

Figure 6. Mimp attenuates HGF/SF-induced cellular scattering. *A,* representative micrographs of iMimp-DA3 and noninducible DA3 cells in grown for 2 days in the presence and absence of 500 ng/mL doxycycline and then in the presence of 2 units/mL HGF/SF. *B,* iMimp-DA3 were grown in absence of doxycycline with and without HGF/SF for 24 hours. The cells were subjected to immunofluorescence analysis using anti–cytokeratin 19 antibodies. *C,* iMimp-DA3 were grown in presence of different doxycycline concentrations for 2 days and then replated in presence of HGF/SF for additional 24 hours. The cells were subjected to immunofluorescence as in (*B*).

Downloaded from http://aacrjournals.org/cancerres/article-pdf/66/17/8687/2552059/8687.pdf by guest on 05 March 2024

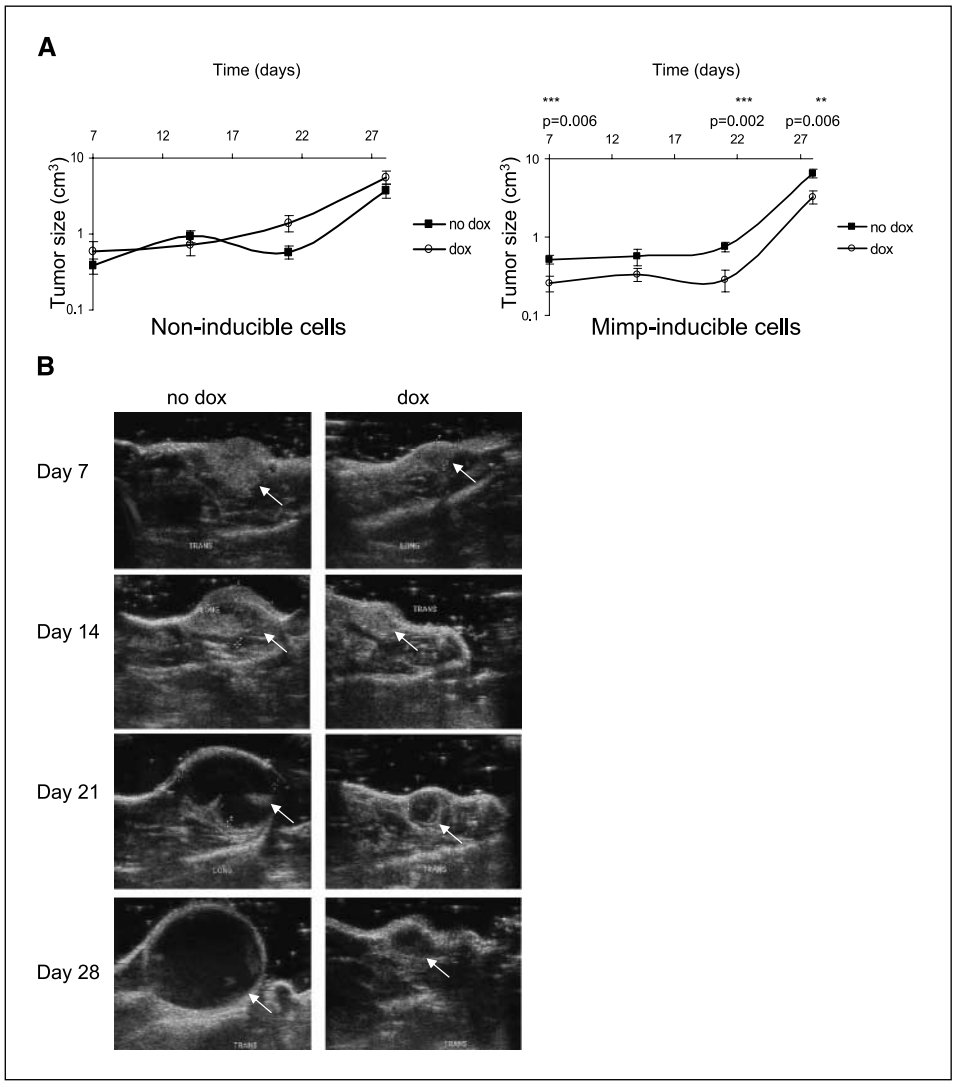

Figure 7. Mimp induction inhibits tumor growth *in vivo*. *A,* iMimp-DA3 and DA3 cells were injected into the mammary pads of female BALB/C mice, which were then divided arbitrarily into two groups, one receiving regular drinking water and the other receiving doxycycline-containing water. Tumor growth was assessed independently and blindly by sonographic measurements once weekly. Average tumor size as assessed by the ultrasound measurement is depicted for both cell lines with and without doxycycline. *B,* representative micrographs of the sonographic visualization of the tumors are seen for a control mouse and for a mouse receiving doxycycline. *Arrows,* tumor in each of the micrographs.

subgroups, one receiving regular drinking water and the other receiving drinking water containing 2 mg/mL doxycycline. The development of mammary tumors was monitored once weekly by caliper measurement and ultrasonographic measurement. Addition of doxycycline to the drinking water did not affect tumor growth rate in the noninducible DA3 cells as assessed by ultrasonographic measurement (Fig. 7*A, left*). In contrast, in the Mimp-inducible cells, the tumors in the group receiving doxycycline grew significantly slower than in the control group (Fig. 7*A, right*). For each time point, the average tumor size of the group receiving doxycycline was 30% (P = 0.002) to 60% (P = 0.006) of the control group. In addition, the tumors from the control group ruptured on average earlier than tumors of the mice receiving doxycycline, indicating that necrosis of the tumor mass occurred earlier in the control group than in the group receiving doxycycline. The complementary approach of caliper measurements of tumor size yielded similar results (results not shown). Representative micrographs from the ultrasonographic imaging of tumors from iMimp-DA3 cells are seen (Fig. 7*B*), which show that the tumor of the mouse receiving regular drinking water was significantly larger at each time point than the tumor of the mouse receiving doxycycline.

Induction of Mimp alters Met-HGF/SF-induced signaling. The differential response to HGF/SF in the presence of Mimp motivated us to check the expression and phosphorylation levels of several known signaling molecules downstream of Met. iMimp-DA3 cells were treated with different concentrations of doxycycline for 2 days, serum starved for 24 hours, and then treated with HGF/SF for 20 minutes. The protein levels and the extent of their phosphorylation were assessed by Western blot analysis or immunoprecipitation followed by Western blot, respectively (Fig. 8*A*). The results were quantified by densitometry and normalized relative to noninduced nontreated cells (Fig. 8*B*).

We observed a dose-dependent increase of Met protein levels as a result of Mimp induction (Fig. 8, *top*). In addition, the levels of phosphorylated Met in response to HGF/SF were higher in Mimp-induced cells relative to noninduced cells, although the basal levels of phosphorylated Met were similar in all three conditions (Fig. 8*A, top*). The attenuation in the HGF/SF-induced cellular response could not therefore be attributed to a decrease in the initial phosphorylation of the Met receptor.

Grb2 was phosphorylated in response to HGF/SF treatment. Induction of Mimp decreased the basal level of phosphorylated Grb2 in a dose-dependent manner. It also prevented the

Downloaded from http://aacrjournals.org/cancerres/article-pdf/66/17/8687/2552059/8687.pdf by guest on 05 March 2024

HGF/SF-induced elevation of phosphorylated Grb2 (Fig. 8*B, middle*). The levels of the Shc adapter protein were decreased in the presence of both concentrations of doxycycline, and its phosphorylated form was decreased following Mimp induction at 500 ng/mL doxycycline (Fig. 8*B, middle*). In the parental DA3 cells, there was no change in the levels of Shc or phosphorylated Shc in the presence of 100 and 500 ng/mL doxycycline (results not shown).

In contrast, an increase in the levels of PI3K was observed following Mimp induction. The basal level of PI3K phosphorylation was reduced in Mimp-induced cells, but it returned to control levels following HGF/SF treatment at both doxycycline concentrations (Fig. 8*B, bottom*). All these results were obtained with the same two membranes, thus ruling out the possibility that these differences stem from differences in the extent of protein loading.

To study whether the decrease in the levels of signaling molecules in presence of Mimp is due to transcriptional regulation, iMimp-DA3 cells were transiently transfected with a vector containing the reporter gene luciferase under a promoter containing SRE. As shown previously, HGF/SF induced expression from the SRE-LUC vector (30). Induction of Mimp prevented the HGF/SF-induced SRE-LUC expression (Fig. 8*C*).

Discussion

In this work, we use an inducible system of Mimp expression in DA3 adenocarcinoma cells. In this model system, there is a tight regulation on the induction of the Mimp protein in response to doxycycline and HGF/SF that is not seen at the transcriptional level. As a consequence, the levels of the inducible protein in our system are very similar to its endogenous levels in response to induction by HGF/SF. The mechanism of such post-transcriptional regulation is currently not known. Interestingly, a discrepancy between mRNA and protein expression levels was also described for UCP2 and UCP3, two other proteins from the mitochondrial carrier family (31, 32), and the existence of post-transcriptional mechanisms that regulate the expression of UCP2 and UCP3 was proposed (31, 32). The tight post-transcriptional regulation on the expression of Mimp, UCP2, UCP3, and possibly other carriers may indicate the importance of maintaining an adequate amount of these proteins in the cell.

The work presented here characterizes the effects of Mimp induction on the biological responses of DA3 cells to HGF/SF. Induction of Mimp does not decrease cell proliferation rate and only slightly elongates the cellular doubling time but does lead to a

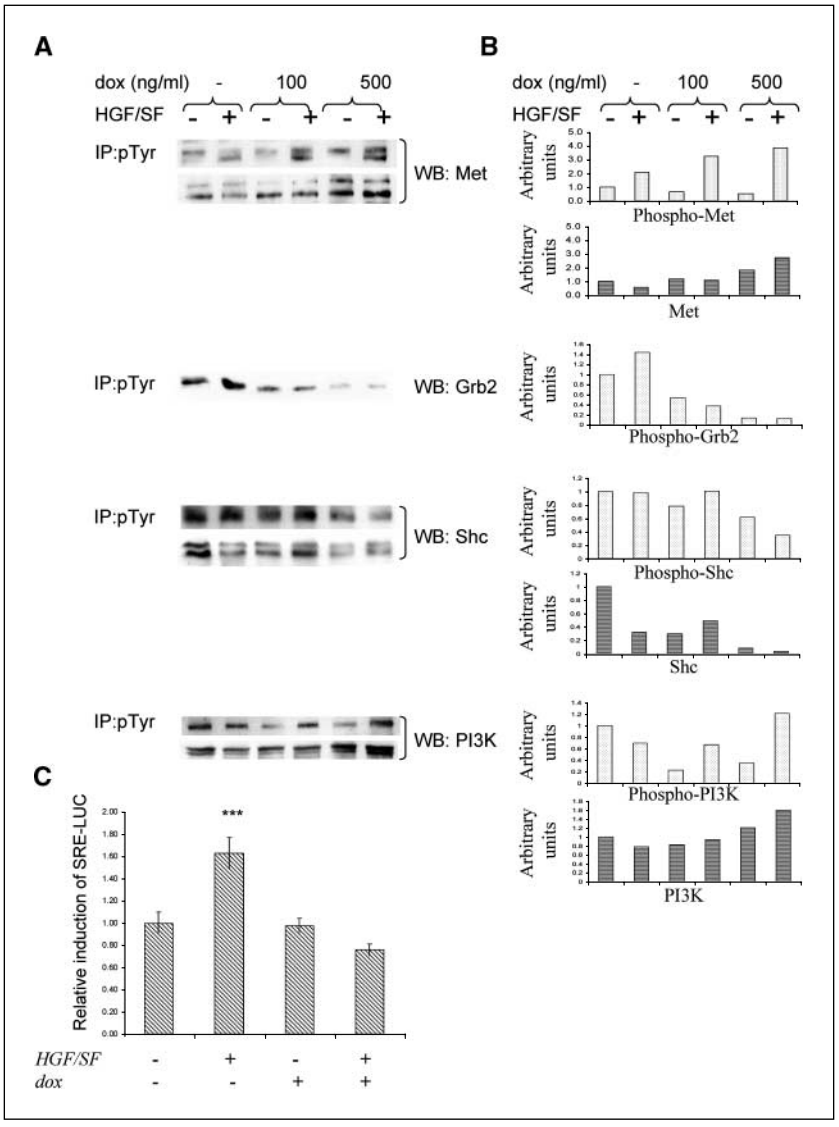

Figure 8. Effect of Mimp induction on Met signaling cascade. *A,* iMimp-DA3 cells were grown in presence of 100 or 500 ng/mL doxycycline for 2 days. Cells were serum deprived for 24 hours, treated with HGF/SF for 20 minutes, and then lysed. Cell lysates were subjected to immunoprecipitation using anti-phosphotyrosine antibody and then to Western blot using anti-Met, anti-Grb2, anti-Shc, and anti-PI3K antibodies. The same lysates were subjected to Western blot using anti-Met, anti-Shc, and anti-PI3K antibodies. The results presented were all derived from the same two membranes following repeated strippings. *B,* densitometric quantification of the Western blot results presented in (*A*). For each blot, the results were normalized relative to nontreated noninduced cells. *C,* iMimp-DA3 cells were transiently transfected with a *SRE-LUC* vector and a *Renilla* vector and then treated with doxycycline and HGF/SF. The luciferase activity was read using a luminometer, normalized relative to the Renilla activity, averaged, and compared with the nontreated cells. ***, $P < 0.005$, one-way ANOVA.

Downloaded from http://aacrjournals.org/cancerres/article-pdf/66/17/8687/2552059/8687.pdf by guest on 05 March 2024

profound change in the response to HGF/SF in terms of growth. HGF/SF has a mild proliferative effect in control cells, but when Mimp is exogenously induced, HGF/SF leads to a significant decrease in cell number and a significant elongation of the doubling time. In addition, Mimp induction significantly decreases tumor growth *in vivo*. Cell cycle analysis shows that in the absence of Mimp induction, HGF/SF drives cells to S phase and to active DNA synthesis. This result is in agreement with the mild proliferative effect of HGF/SF in this system. In contrast, in the presence of Mimp, addition of HGF/SF leads to accumulation of cells at the S phase that cells are not actively synthesizing DNA or are synthesizing DNA at a much lower rate.

Although several factors are known to lead to S-phase arrest or to S-phase elongation, growth arrest in the S phase of the cell cycle is poorly understood. We show that the mRNA and protein levels of cdc2 increase in response to HGF/SF but significantly decrease in response to HGF/SF in presence of Mimp, whereas the levels of the cell cycle inhibitors p21 and p27 are increased following Mimp induction. A decrease in cdc2 has been reported in cell cycle delays in response to ionizing radiation (33) and in response to the toxin malondialdehyde (34). In both cases, the decrease in cdc2 was accompanied by an increase in the levels of the p21 inhibitor (33, 34). In addition, a significant decrease in total cdc2 protein was observed in prostate cancer cells following incubation with IGFBP3, which also leads to a significant reduction in [^{3}H]thymidine incorporation and to an increase in the percentage of cells in the S phase (35). Last, the cancer drug STI571 was shown to lead to accumulation of cells at the S and G_2-M phases of the cell cycle in anaplastic thyroid cancer cells in a mechanism that involved both a decrease in cdc2 protein and an increase in p21 and p27 (36). The alterations in the cell cycle proteins and the S-phase arrest in response to Mimp can explain the observed elongation of the doubling time and the decrease in cell growth in response to HGF/SF. To our knowledge, our results are the first to show S-phase arrest following induction of a mitochondrial protein.

The observation that exogenous induction of Mimp attenuates the proliferative response to HGF/SF in DA3 brought us to check its endogenous levels in cell systems that differ in their proliferative response to HGF/SF. Interestingly enough, the cell line that responded to HGF/SF in proliferation had significantly lower levels of Mimp than the three cell lines that responded to HGF/SF in growth arrest. This correlative observation may suggest that the basal levels of Mimp might be one of the variables that affect the nature of the cellular response to HGF/SF either directly or indirectly.

Currently, little is known about the involvement of proteins from the mitochondrial carrier superfamily in cellular transformation. This work shows for the first time that induction of a mitochondrial carrier protein homologue that is not in itself toxic to cells inhibits tumor growth. mtch1, the mitochondrial carrier homologue most similar to Mimp, is a proapoptotic protein (16). In contrast to mtch1, Mimp does not lead to apoptosis. Moreover, HGF/SF has an antiapoptotic effect in DA3 cells as has also been described for other cells (8, 37, 38), and this effect is preserved in the presence of Mimp. In addition, Mimp expression does not render cells more susceptible to apoptosis by UV irradiation and does not lead to cytochrome *c* release from the mitochondria. Overexpression of Mimp in 293T cells does not lead to apoptosis, although it does lead to depolarization of the mitochondria.

Mimp also inhibits HGF/SF-induced scattering, because in its presence the concentrations of HGF/SF needed for scattering are higher than in its absence. The process of cell scattering includes the phases of cell spreading, cell-cell dissociation, and cell migration. Disassembly of cell-cell junctions occurs during certain physiologic conditions throughout development as well as under pathologic circumstances, such as tumor invasion and metastasis (1). Thus far, a mitochondrial protein has not been implicated in inhibition of cellular scattering.

Induction of Mimp at levels similar to its physiologic induction by HGF/SF leads to profound changes in the total levels of several signaling molecules downstream of Met and in their phosphorylation patterns. The levels of Shc are decreased when Mimp is induced, and the extent of its tyrosine phosphorylation is greatly reduced following induction of Mimp with or without HGF/SF treatment. Shc is a substrate of Met and works as an amplifier of the motogenic as well as of the mitogenic response to HGF/SF (6). Shc also recruits Grb2 to Met (6). Grb2, an important adaptor protein for Met-HGF/SF, was found to mediate many of the HGF/SF-induced responses (5, 39), especially proliferation (40), by binding either directly to the docking site of Met or through Shc (6). Grb2 is phosphorylated in response to HGF/SF in DA3 cells. The induction of Mimp reduces the extent of Grb2 phosphorylation in a dose-dependent manner. It was shown that antagonists to Grb2-SH2 domain interactions lead to potent blockade of HGF/SF-stimulated cell motility, matrix invasion, and branching morphogenesis (41). The induction of Mimp leads to a similar alteration in Grb2 signaling and to a similar attenuated response to HGF/SF. In contrast, Mimp induction increases both the levels of Met and the extent of its phosphorylation in response to HGF/SF. These results indicate that the Mimp-induced effects on the signaling pathway occur downstream of the receptor.

The levels of the protein PI3K are elevated when Mimp is induced. Following Mimp induction, PI3K phosphorylation is decreased but increases to control levels following HGF/SF treatment. It therefore seems that the cell "maintains" steady-state levels of phosphorylated PI3K in presence of both low and high levels of Mimp by elevating the basal protein levels. PI3K has been implicated in the antiapoptotic response to HGF/SF in several cell types (8). We propose that the maintenance of a constant level of phosphorylated PI3K in the presence of HGF/SF and Mimp is part of what allows the preservation of the antiapoptotic effect of HGF/SF in the presence of Mimp.

Activation of Met by HGF/SF leads to activation of the downstream signaling pathway of Ras-Raf-1-Erk1/Erk2-Elk-1, the last being a transcription factor that binds to SRE (30). This signaling pathway is well known to be involved in cellular proliferation, and it has been shown in the past that HGF/SF induces the expression of SRE-LUC in HeLa cells (30). We show a similar induction of SRE-LUC in response to HGF/SF, which disappears in presence of Mimp. This observation may suggest that the effect of Mimp is exerted, at least in part, by transcriptional repression.

In summary, our current work suggests that induction of exogenous Mimp at the mitochondria leads to alterations in the transcription from SRE-containing promoters, thus changing the expression pattern of signaling molecules. These effects of Mimp lead to the observed decrease in growth and in motility in response to HGF/SF without leading to apoptosis. We hypothesize that the endogenous induction of Mimp by Met-HGF/SF serves as a negative regulatory mechanism that restrains their signaling,

Downloaded from http://aacrjournals.org/cancerres/article-pdf/66/17/8687/2552059/8687.pdf by guest on 05 March 2024

thus lowering the potential harmful outcome of activation of this receptor.

Met is overexpressed in many human tumors (1, 42) and is a potential target for antitumor therapy (1). Identifying proteins that serve as natural negative regulators of this important signaling pathway may shed light on the molecular mechanisms of Met-induced tumorigenicity and metastasis and may aid in finding efficient ways to block this activity.

Acknowledgments

Received 6/30/2005; revised 5/22/2006; accepted 6/23/2006.

Grant support: Israel Science Foundation (founded by the Israel Academy of Sciences and Humanities) and NIH research grant P50CA93990.

The costs of publication of this article were defrayed in part by the payment of page charges. This article must therefore be hereby marked *advertisement* in accordance with 18 U.S.C. Section 1734 solely to indicate this fact.

We thank Mary Beth Bruch (Van Andel Research Institute) for outstanding ultrasound analysis and Dr. Yitzchak Oschry (Interdepartmental Core Facility at the Sackler School of Medicine) for excellent assistance with the FACS.

References

1. Maulik G, Shrikhande A, Kijima T, Ma PC, Morrison PT, Salgia R. Role of the hepatocyte growth factor receptor, c-Met, in oncogenesis and potential for therapeutic inhibition. Cytokine Growth Factor Rev 2002;13:41–59.
2. Jiang WG, Martin TA, Parr C, Davies G, Matsumoto K, Nakamura T. Hepatocyte growth factor, its receptor, and their potential value in cancer therapies. Crit Rev Oncol Hematol 2005;53:35–69.
3. Comoglio PM. Pathway specificity for Met signalling. Nat Cell Biol 2001;3:E161–2.
4. Lamorte L, Royal I, Naujokas M, Park M. Crk adapter proteins promote an epithelial-mesenchymal-like transition and are required for HGF-mediated cell spreading and breakdown of epithelial adherens junctions. Mol Biol Cell 2002;13:1449–61.
5. Furge KA., Zhang YW, Vande Woude GF. Met receptor tyrosine kinase: enhanced signaling through adapter proteins. Oncogene 2000;19:5582–9.
6. Pelicci G, Giordano S, Zhen Z, et al. The motogenic and mitogenic responses to HGF are amplified by the Shc adaptor protein. Oncogene 1995;10:1631–8.
7. Maroun CR, Holgado-Madruga M, Royal I, et al. The Gab1 PH domain is required for localization of Gab1 at sites of cell-cell contact and epithelial morphogenesis downstream from the Met receptor tyrosine kinase. Mol Cell Biol 1999;19:1784–99.
8. Xiao GH, Jeffers M, Bellacosa A, Mitsuuchi Y, Vande Woude GF, Testa JR. Anti-apoptotic signaling by hepatocyte growth factor/Met via the phosphatidylinositol 3-kinase/Akt and mitogen-activated protein kinase pathways. Proc Natl Acad Sci U S A 2001;98:247–52.
9. Yerushalmi GM, Leibowitz-Amit R, Shaharabany M, Tsarfaty I. Met-HGF/SF signal transduction induces mimp, a novel mitochondrial carrier homologue, which leads to mitochondrial depolarization. Neoplasia 2002;4:510–22.
10. Zhang QH, Ye M, Wu XY, et al. Cloning and functional analysis of cDNAs with open reading frames for 300 previously undefined genes expressed in CD34$^+$ hematopoietic stem/progenitor cells. Genome Res 2000;10:1546–60.
11. Stanton JL, Green DP. A set of 1542 mouse blastocyst and pre-blastocyst genes with well-matched human homologues. Mol Hum Reprod 2002;8:149–66.
12. Taylor SW, Fahy E, Zhang B, et al. Characterization of the human heart mitochondrial proteome. Nat Biotechnol 2003;21:281–6.
13. Rome S, Clement K, Rabasa-Lhoret R, et al. Microarray profiling of human skeletal muscle reveals that insulin regulates ~800 genes during a hyperinsulinemic clamp. J Biol Chem 2003;278:18063–8.
14. Grinberg M, Schwarz M, Zaltsman Y, et al. Mitochondrial carrier homolog 2 is a target of tBID in cells signaled to die by tumor necrosis factor α. Mol Cell Biol 2005;25:4579–90.
15. Xu X, Shi Y, Wu X, Gambetti P, Sui D, Cui MZ. Identification of a novel PSD-95/Dlg/ZO-1 (PDZ)-like protein interacting with the C terminus of presenilin-1. J Biol Chem 1999;274:32543–6.
16. Xu X, Shi YC, Gao W, et al. The novel presenilin-1-associated protein is a proapoptotic mitochondrial protein. J Biol Chem 2002;277:48913–22.
17. Fu Y, Watson G, Jimenez JJ, Wang Y, Lopez DM. Expansion of immunoregulatory macrophages by granulocyte-macrophage colony-stimulating factor derived from a murine mammary tumor. Cancer Res 1990;50:227–34.
18. Rong S, Oskarsson M, Faletto D, et al. Tumorigenesis induced by coexpression of human hepatocyte growth factor and the human met protooncogene leads to high levels of expression of the ligand and receptor. Cell Growth Differ 1993;4:563–9.
19. Harlow E, Lane D. Antibodies: a laboratory manual. Cold Sprint Harbor (NY): Cold Spring Harbor Laboratory Press; 1988.
20. Kueng W, Silber E, Eppenberger U. Quantification of cells cultured on 96-well plates. Anal Biochem 1989;182:16–9.
21. Benussi L, Alberici A, Mayhaus M, et al. Detection of the presenilin 1 COOH-terminal fragment in the extracellular compartment: a release enhanced by apoptosis. Exp Cell Res 2001;269:256–65.
22. Rosen EM, Goldberg ID, Kacinski BM, Buckholz T, Vinter DW. Smooth muscle releases an epithelial cell scatter factor which binds to heparin. In Vitro Cell Dev Biol 1989;25:163–73.
23. Stoker M, Gherardi E, Perryman M, Gray J. Scatter factor is a fibroblast-derived modulator of epithelial cell mobility. Nature 1987;327:239–42.
24. Sambrook J, Fritsch EF, Maniatis T. Molecular cloning: a laboratory manual. Cold Spring Harbor (NY): Cold Spring Harbor Laboratory Press; 1989.
25. Salvioli S, Ardizzoni A, Franceschi C, Cossarizza A. JC-1, but not DiOC6(3) or rhodamine 123, is a reliable fluorescent probe to assess δψ changes in intact cells: implications for studies on mitochondrial functionality during apoptosis. FEBS letters 1997;411:77–82.
26. Green DR, Reed JC. Mitochondria and apoptosis. Science 1998;281:1309–12.
27. Firon M, Shaharabany M, Altstock RT, et al. Dominant negative Met reduces tumorigenicity-metastasis and increases tubule formation in mammary cells. Oncogene 2000;19:2386–97.
28. Chu PG, Weiss LM. Keratin expression in human tissues and neoplasms. Histopathology 2002;40:403–39.
29. Dugina VB, Alexandrova AY, Lane K, Bulanova E, Vasiliev JM. The role of the microtubular system in the cell response to HGF/SF. J Cell Sci 1995;108:1659–67.
30. Wang D, Li Z, Messing EM, Wu G. The SPRY domain-containing SOCS box protein 1 (SSB-1) interacts with MET and enhances the hepatocyte growth factor-induced Erk-Elk-1-serum response element pathway. J Biol Chem 2005;280:16393–401.
31. Sivitz WI, Fink BD, Donohoue PA. Fasting and leptin modulate adipose and muscle uncoupling protein: divergent effects between messenger ribonucleic acid and protein expression. Endocrinology 1999;140:1511–9.
32. Pecqueur C, Alves-Guerra MC, Gelly C, et al. Uncoupling protein 2, *in vivo* distribution, induction upon oxidative stress, and evidence for translational regulation. J Biol Chem 2001;276:8705–12.
33. De Toledo SM, Azzam EI, Keng P, Laffrenier S, Little JB. Regulation by ionizing radiation of CDC2, cyclin A, cyclin B, thymidine kinase, topoisomerase IIα, and RAD51 expression in normal human diploid fibroblasts is dependent on p53/p21Waf1. Cell Growth Differ 1998;9:887–96.
34. Ji C, Rouzer CA, Marnett LJ, Pietenpol JA. Induction of cell cycle arrest by the endogenous product of lipid peroxidation, malondialdehyde. Carcinogenesis 1998;19:1275–83.
35. Manes S, Llorente M, Lacalle RA, et al. The matrix metalloproteinase-9 regulates the insulin-like growth factor-triggered autocrine response in DU-145 carcinoma cells. J Biol Chem 1999;274:6935–45.
36. Podtcheko A, Ohtsuru A, Tsuda S, et al. The selective tyrosine kinase inhibitor, STI571, inhibits growth of anaplastic thyroid cancer cells. J Clin Endocrinol Metab 2003;88:1889–96.
37. Bowers DC, Fan S, Walter KA, et al. Scatter factor/hepatocyte growth factor protects against cytotoxic death in human glioblastoma via phosphatidylinositol 3-kinase- and AKT-dependent pathways. Cancer Res 2000;60:4277–83.
38. Gao M, Fan S, Goldberg ID, Laterra J, Kitsis RN, Rosen EM. Hepatocyte growth factor/scatter factor blocks the mitochondrial pathway of apoptosis signaling in breast cancer cells. J Biol Chem 2001;276:47257–65.
39. Saucier C, Papavasiliou V, Palazzo A, Naujokas MA, Kremer R, Park M. Use of signal specific receptor tyrosine kinase oncoproteins reveals that pathways downstream from Grb2 or Shc are sufficient for cell transformation and metastasis. Oncogene 2002;21:1800–11.
40. Leshem Y, Gitelman I, Ponzetto C, Halevy O. Preferential binding of Grb2 or phosphatidylinositol 3-kinase to the met receptor has opposite effects on HGF-induced myoblast proliferation. Exp Cell Res 2002;274:288–98.
41. Atabey N, Gao Y, Yao ZJ, et al. Potent blockade of hepatocyte growth factor-stimulated cell motility, matrix invasion and branching morphogenesis by antagonists of Grb2 Src homology 2 domain interactions. J Biol Chem 2001;276:14308–14.
42. Haddad R, Lipson KE, Webb CP. Hepatocyte growth factor expression in human cancer and therapy with specific inhibitors. Anticancer Res 2001;21:4243–52.

Downloaded from http://aacrjournals.org/cancerres/article-pdf/66/17/8687/2552059/8687.pdf by guest on 05 March 2024